Acoustic wave propagation in structurally helical media

C. Oldano and S. Ponti
Dipartimento di Fisica del Politecnico di Torino and Istituto Nazionale di Fisica della Materia, C.so Duca degli Abruzzi 24, 10129 Torino, Italy

(Received 20 January 2000; revised manuscript received 12 July 2000; published 18 December 2000)

A theoretical analysis is given of the acoustic wave propagation in periodically nonhomogeneous media made of a solid material whose stiffness tensor is uniformly rotating along a given axis. In the last years, such media have been studied theoretically as well as experimentally, in particular for what concerns sample preparation and possible applications. A detailed analysis of their acoustical properties is given here, based on fully analytic and simple propagation equations. For axial propagation: (i) the dispersion curves of media where the transversal field components and the longitudinal ones are not coupled show only one forbidden band, that gives selective Bragg diffraction; in the opposite case they show at least a second forbidden band, that involves the quasilongitudinal and one of the quasitransversal eigenmodes; (ii) in the first case (absence of coupling), the medium gives pure acoustical rotation for $p \ll \lambda$, where p is the helical pitch and λ the acoustical wavelength, a nonperfectly uniform but very large rotatory power for p of the order of λ, and a guided rotation for $p \gg \lambda$; (iii) in the presence of the coupling, regions of mode exchange between the longitudinal component and a transversal one are generally present. The cases of lossy media and of quasiaxial propagation are also considered, and the analogies between optical and acoustical properties discussed.

DOI: 10.1103/PhysRevE.63.011703 PACS number(s): 61.30.−v, 62.65.+k

I. INTRODUCTION

Very few periodic media have attracted as much interest in optics as cholesteric liquid crystals, where the optic axis of an uniaxial material is uniformly rotating in space along a given direction, say x_3, being everywhere orthogonal to x_3. There are many good reasons for such interest: these structurally helical media are very simple and at the same time important, because frequently found in nature, easily obtained artificially and of great interest for their properties. We recall in particular the following facts. For light propagating along the axis x_3 (axial propagation) the Maxwell equations admit fully analytic and very simple solutions. In a coordinate system whose axes x_1 and x_2 rotate in space, rigidly following the rotation of the optic axis, such solutions assume the simple form of plane waves. In this sense and in this geometry the inhomogeneous medium behaves therefore as homogeneous, with unusual and interesting optical properties that can be drastically changed by changing the helix pitch and the optical anisotropy.

Even more interesting properties are expected for the propagation of acoustic waves in solid helical media. In the last decade such waves have been the object of intense research, in particular by Lakhtakia and co-workers, in the following directions.

(i) Theoretical analysis of acoustic wave propagation in solid helical media without [1–3] and with [4–6] piezoelectric coupling between the acoustic and the electromagnetic fields.

(ii) Study of possible application [7–10].

(iii) Improvements of the already known techniques for the preparation of helical samples, and developments of new techniques [11–14].

Helical liquid crystals are of little usefulness for acoustical applications, because they behave as inhomogeneous liquids with high viscosity. It is however possible, at least in principle, to obtain suitable samples by freezing an high temperature liquid crystal, to obtain a metastable phase able to support elastic shear waves. In the following, we will make reference to N^*-like and C^*-like structures, which behave acoustically as frozen cholesterics (or chiral nematics, N^*) and chiral C-smectics (C^*), and have very different acoustical properties.

The aim of the paper is the theoretical analysis of the eigenmodes for the acoustic wave propagation in a continuously twisted solid medium, in the absence of piezoelectricity. For axial propagation, it is convenient to separately consider the cases without and with coupling between the longitudinal and transversal components of the displacement vector, which correspond respectively, to N^*- and C^*-like structures. The first case has already been considered in Refs. [1,3,7,8]. Some not yet fully explored properties of the eigenmodes are discussed in Sec. III, that can therefore be considered as a continuation of the cited papers. The other case has received less attention up as yet, and constitutes the most original part of the paper. The case of oblique propagation has been treated in Refs. [5,6], so that only the simple case of quasiaxial propagation is considered.

II. BASIC DEFINITIONS AND PROPAGATION EQUATIONS

A. Definition of the system

Before the discovery of cholesteric liquid crystals, Reusch [15] prepared and studied the first artificial helical object, by superposing layers of mica and progressively changing their orientation along the stack (Reusch pile). We consider a Reusch pile made of identical anisotropic thin sheets of thickness d, each one rotated of an angle $\Delta\phi$ with respect to the preceding one, and define in any sheet a local Cartesian frame whose axis x_3 is orthogonal to the sheets, and whose axes x_1 and x_2 are such that the elastic tensor components

$\tilde{\lambda}_{lijm}$ of the stiffness tensor $\underline{\lambda}$ have the same values in all the sheets. In the limit where both d and $\Delta\phi$ go to zero with a fixed value of the ratio $q=\Delta\phi/d$, the axes x_1 and x_2 rotate in space describing helices with a pitch

$$p=2\pi/q. \tag{1}$$

The helices are right-handed for $q>0$, left-handed for $q<0$. We define then a laboratory (nonrotating) frame x_1',x_2',x_3', with $x_3'=x_3$, and a rotation matrix $\underline{R}$ such that

$$x_i'=R_{ij}x_j, \quad i,j=1,2,3. \tag{2}$$

An external monocromatic plane wave with wave vector $\vec{k}'$ lying in the plane x_1', x_3' generates internal waves whose wave vectors have tangential component $\vec{k}_1'\cdot\hat{x}_1'$ (phase matching condition). The displacement vector $\vec{u}$ and the stress tensor $\underline{\sigma}$ in the rotating frame can be written as

$$\begin{aligned} u_l&=u_l(x_3)\exp[i(k_1'x_1'-\omega t)],\\ \sigma_{lm}&=\sigma_{lm}(x_3)\exp[i(k_1'x_1'-\omega t)]. \end{aligned} \tag{3}$$

The propagation equations for the displacement vector and for the stress tensor in both the laboratory and the rotating frame are given in Refs. [4,6] for the more general case of piezoelectric crystals in a very compact but implicit form. Rather long but simple calculations give the following explicit propagation equation in the rotating frame:

$$\frac{d\vec{\beta}}{dx_3}=i\underline{B}\vec{\beta}, \tag{4}$$

$$\vec{\beta}=\begin{bmatrix}\vec{u}\\ \vec{\sigma}\end{bmatrix}, \quad \underline{B}=\begin{bmatrix}\underline{B}_{uu} & \underline{B}_{u\sigma}\\ \underline{B}_{\sigma u} & \underline{B}_{\sigma\sigma}\end{bmatrix},$$

where $\sigma_j=\sigma_{j3}$, and the kernel matrix B is defined by the following set of equations:

$$i\underline{B}_{uu}=q\underline{r}-ik_1'\underline{\eta}(\underline{\tilde{\lambda}}^{31}\cos\phi-\underline{\tilde{\lambda}}^{32}\sin\phi), \tag{5}$$

$$i\underline{B}_{u\sigma}=\underline{\eta},$$

$$i\underline{B}_{\sigma u}=-\rho\omega^2\mathbb{1}-ik_1'[\underline{a}_{11}\cos\phi-\underline{a}_{21}\sin\phi],$$

$$i\underline{B}_{\sigma\sigma}=-q\underline{r}-ik_1'[\underline{a}_{12}\cos\phi-\underline{a}_{22}\sin\phi],$$

$$a_{j1}=ik_1'\underline{\eta}[(\underline{\tilde{\lambda}}^{j1}-\underline{\tilde{\lambda}}^{j3}\underline{\eta}\underline{\tilde{\lambda}}^{31})\cos\phi-(\underline{\tilde{\lambda}}^{j2}-\underline{\tilde{\lambda}}^{j3}\underline{\eta}\underline{\tilde{\lambda}}^{32})\sin\phi], \tag{6}$$

$$a_{j2}=\underline{\tilde{\lambda}}^{j3}\underline{\eta},$$

where $j=1,2$; $\underline{\tilde{\lambda}}^{ij}$ and $\underline{\eta}$ are 3×3 matrices defined as

$$\tilde{\lambda}^{ij}_{lm}=\tilde{\lambda}_{lijm}, \quad \underline{\eta}=(\underline{\tilde{\lambda}}^{33})^{-1}; \tag{7}$$

$\mathbb{1}$ is the 3×3 identity matrix;

$$\underline{r}=\begin{pmatrix}0 & -1 & 0\\ 1 & 0 & 0\\ 0 & 0 & 0\end{pmatrix} \tag{8}$$

and

$$\phi=qx_3+\phi_0. \tag{9}$$

Only three components of the stress tensor $\underline{\sigma}$ appear in the propagation equation, and the 6×6 kernel matrix $\underline{B}$ depends on x_3 only through the azimuthal angle ϕ that defines the rotation of the local axes x_1, x_2 with respect to x_1', x_2'. Since the angle ϕ only appears in the terms depending on k_1', the kernel matrix $\underline{B}$ is *independent of* x_3 for $k_1'=0$, i.e., for *axial propagation*. This is the main advantage of the rotating frame with respect to the laboratory one. Further, for small k_1' values, i.e., at quasiaxial propagation, the x_3-dependent terms can be treated perturbatively.

In Refs. [5,6] the 6×6 stiffness matrix C instead of the fourth rank tensor λ is considered. An alternative derivation of the propagation equations, that avoids the use of the matrix C, is given in the Appendix.

It is important to observe that the axes (x_1,x_2,x_3), used here to express the components of the stiffness tensors in any sheet, are different from the crystallographic axes (x,y,z) generally used in the theory of elasticity [16]. A further rotation matrix is therefore required to relate the components $\tilde{\lambda}_{ijkl}$ and λ_{ijkl} of the stiffness tensor λ in the rotating and in the crystallographic frames. In the following, we use the symbols $\lambda'_{ijkl}(x_3')$, $\tilde{\lambda}_{ijkl}$, and λ_{ijkl} for the components of the tensor $\underline{\lambda}$ in the laboratory, rotating and crystallographic frames, respectively (similarly for the components of C).

The medium will be assumed as lossless and achiral, and therefore defined by a real symmetric matrix C, except in the Sec. III C, where a brief discussion of the possible effects of losses is given.

B. Axial propagation: Cholestericlike and smecticlike structures

For axial propagation, the 3×3 submatrices of B write

$$B_{uu}=B_{\sigma\sigma}=-iq\underline{r}, \quad B_{u\sigma}=-i\underline{\eta}, \quad B_{\sigma u}=i\rho\omega^2\mathbb{1}. \tag{10}$$

The matrix $\underline{r}$ appearing in B_{uu} and $B_{\sigma\sigma}$ couples the transversal components u_1, u_2, σ_1, σ_2 of the state vector β, whereas the coupling between these components and the longitudinal ones depends on the structure of the matrix $\underline{\eta}=(\underline{\tilde{\lambda}}^{33})^{-1}$. As already stated in the introduction, it is convenient to separately treat the cases with and without coupling between transversal (T) and longitudinal (L) components. The decoupling between the T and L components of the state vector only occurs in solid media having a structure similar to the one of cholesteric (N^*) liquid crystals, namely in helical structures that locally have a symmetry axis orthogonal to the helix axis x_3. In all the other helical structures, including smectic C^* liquid crystals, the six components are coupled. As already stated in the introduction, these two

types of structures are referred here as N^*-like and C^*-like, for brevity, but our analysis covers any solid helical structure.

The coupling between T and L components is given by the elements of the symmetric matrices $\underline{\eta}$ and $\underline{\tilde{\lambda}}^{33}$ having pedices 13 and 23. The conditions to obtain N^*-like structures are therefore

$$\tilde{\lambda}_{13}^{33}=\tilde{\lambda}_{1333}=\tilde{C}_{53}=0, \quad \tilde{\lambda}_{23}^{33}=\tilde{\lambda}_{2333}=\tilde{C}_{43}=0. \tag{11}$$

For axial propagation, any plane containing x_3 can be considered as the incidence plane (x_1,x_3). If the conditions (11) are satisfied, a suitable choice of x_1 diagonalizes the matrices $\underline{\tilde{\lambda}}^{33}$ and $\underline{\eta}$. In the N^*-like structures we can therefore set

$$\underline{\eta}=\begin{pmatrix} \eta_1 & 0 & 0 \\ 0 & \eta_2 & 0 \\ 0 & 0 & \eta_3 \end{pmatrix} \tag{12}$$

without loss of generality.

To better understand the meaning of Eq. (11) for structures whose layers are perfect crystals, we must consider the reference frame (x,y,z). If it is coincident with the rotating frame (x_1,x_2,x_3), Eq. (11) is satisfied by crystals of all crystallographic systems, except the triclinic one, which gives in any case C^*-like structures. It is however to be observed that only the monoclinic and orthorombic systems are of interest. In fact the other, more symmetric, systems give a structure that behaves no more as helicoidal: the three components u_1,u_2,u_3 of $\vec{u}$ become uncoupled, and the solutions of the propagation equations are trivial. Such systems (except the cubic one) give interesting structures if the crystallographic axis z makes an angle θ (tilt angle) with the helical axis x_3. In the following sections we consider media whose matrix C in the crystallographic frame (x,y,z) has the simple structure:

$$\underline{C}=\begin{pmatrix} C_{11} & C_{12} & C_{13} & 0 & 0 & 0 \\ C_{12} & C_{22} & C_{23} & 0 & 0 & 0 \\ C_{13} & C_{23} & C_{33} & 0 & 0 & 0 \\ 0 & 0 & 0 & C_{44} & 0 & 0 \\ 0 & 0 & 0 & 0 & C_{55} & 0 \\ 0 & 0 & 0 & 0 & 0 & C_{66} \end{pmatrix}. \tag{13}$$

We recall that in Eq. (13) the indexes have the following meaning:

$$1\leftrightarrow xx, \quad 2\leftrightarrow yy, \quad 3\leftrightarrow zz, \quad 4\leftrightarrow yz, \quad 5\leftrightarrow xz, \quad 6\leftrightarrow xy,$$

and that the stiffness matrix has the structure of Equation (13) for crystals of the cubic, hexagonal, and orthorhombic systems and of the classes $4mm$, 422, $\bar{4}2m$, $4/mm$ of the tetragonal system. Equation (13) is also valid for frozen cholesteric and chiral smectic liquid crystals, which can be considered made of layers having symmetry $D_{\infty h}$ and C_{2h}, respectively (∞/m and $2/m$ in international notations). With such crystals, we obtain a N^*-like structure if the crystallographic axis z is everywhere orthogonal to the helix axis x_3 (i.e., if $\theta=90°$) and a C^*-like structure if it is obliquely oriented. For the sake of definiteness, we will consider in the next section N^*-like structures where $\theta=90°$, $z=x_1$, and $y=x_2$. In this case

$$\eta_1=1/C_{55}, \quad \eta_2=C_{66}, \quad \eta_3=1/C_{11}. \tag{14}$$

As stated in the introduction, the axial propagation in N^*-like structures has been already treated in several papers, so that we only discuss some properties that have not yet been fully explored. Analogies and differences between acoustical and optical waves are evidenced by comparing the acoustical properties of solid helical media with the well-known optical properties of the helical liquid crystal media. To this purpose, we observe that the difference between liquid and solid structures is not very important for the electromagnetic waves, at least in the framework of linear optics, whereas it becomes essential for the acoustic waves.

III. AXIAL PROPAGATION IN CHOLESTERICLIKE STRUCTURES

The propagation matrix $\underline{B}$, given by Eq. (10), is a constant matrix and admits solutions having the simple form of plane waves:

$$\vec{u}=\vec{u}_0\exp(ikx_3), \quad \vec{\sigma}=\vec{\sigma}_0\exp(ikx_3). \tag{15}$$

For N^*-like structures the longitudinal (L) and transversal (T) components of the vectors $\vec{u}$ and $\vec{\sigma}$ are not coupled. The longitudinal components satisfy the equation

$$-i\begin{pmatrix} 0 & \eta_3 \\ -\rho\omega^2 & 0 \end{pmatrix}\begin{pmatrix} u_3 \\ \sigma_3 \end{pmatrix}=k\begin{pmatrix} u_3 \\ \sigma_3 \end{pmatrix}, \tag{16}$$

which gives

$$k^2=\rho\eta_3\omega^2=\rho\omega^2/C_{11}. \tag{17}$$

[As already stated, we consider in this section structures for which η_i are related to C_{ij} by Eq. (14), for the sake of definiteness: for the other N^*-like structures, we must simply substitute C_{11},C_{55},C_{66} with other elastic constants.] The two solutions correspond to eigenmodes propagating in opposite directions (L-modes). These modes have been exhaustively treated in Ref. [3], so that no further analysis is required.

The two transversal components are coupled and satisfy the equation

$$-i\begin{pmatrix} 0 & q & \eta_1 & 0 \\ -q & 0 & 0 & \eta_2 \\ -\rho\omega^2 & 0 & 0 & q \\ 0 & -\rho\omega^2 & -q & 0 \end{pmatrix}\begin{pmatrix} u_1 \\ u_2 \\ \sigma_1 \\ \sigma_2 \end{pmatrix}=k\begin{pmatrix} u_1 \\ u_2 \\ \sigma_1 \\ \sigma_2 \end{pmatrix}, \tag{18}$$

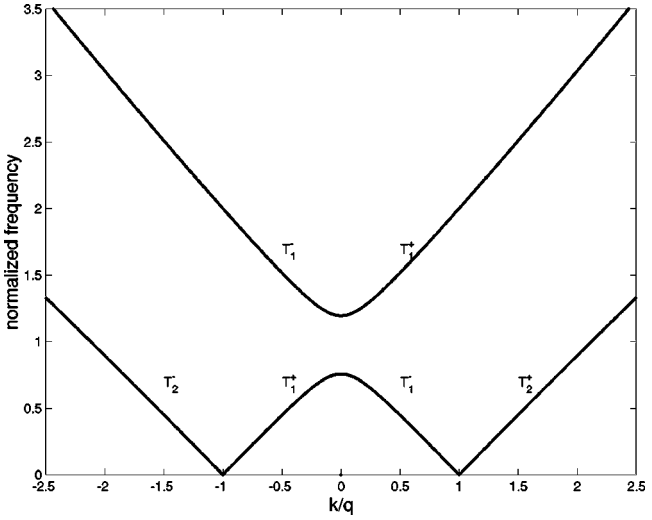

FIG. 1. Dispersion curves in the rotating frame for a cholestericlike structure made of tellurium dioxide (class 422). $C_{55}=2.65$ (10^{10} N/m^2) and $C_{66}=6.59$ (10^{10} N/m^2). The normalization frequency is $q\sqrt{(C_{55}+C_{66})/\rho}$.

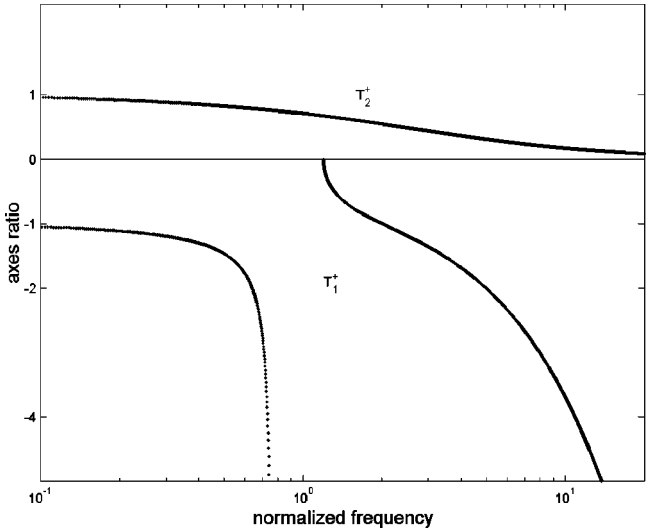

FIG. 2. Axes ratio versus normalized frequency. Within the frequency gap the eigenmode 1^+ is linearly polarized. The material parameters are the same as in Fig. 1.

that summarizes the properties of the four transversal eigenmodes T_1^+, T_2^+, T_1^-, and T_2^-. After elimination of the components σ_1 and σ_2, we obtain the equation system

$$\begin{pmatrix} C_{55}k^2+C_{66}q^2 & iqk(C_{55}+C_{66}) \\ -iqk(C_{55}+C_{66}) & C_{66}k^2+C_{55}q^2 \end{pmatrix}\begin{pmatrix} u_1 \\ u_2 \end{pmatrix}=\rho\omega^2\begin{pmatrix} u_1 \\ u_2 \end{pmatrix}, \tag{19}$$

which straightforwardly gives

$$k^2=q^2+k_{\rm int}^2\pm\sqrt{4q^2k_{\rm int}^2+k_{\rm int}^4\delta^2}, \tag{20}$$

$$\frac{u_2}{u_1}=\frac{-iqk(C_{55}+C_{66})}{C_{55}k^2+C_{66}q^2-\rho\omega^2}\equiv\frac{C_{55}q^2+C_{66}k^2-\rho\omega^2}{iqk(C_{55}+C_{66})}, \tag{21}$$

where

$$k_{\rm int}^2=\rho\omega^2\frac{C_{55}+C_{66}}{2C_{55}C_{66}},\qquad \delta=\frac{C_{55}-C_{66}}{C_{55}+C_{66}}. \tag{22}$$

The parameter $k_{\rm int}$ has the meaning of an averaged wave vector. Equation (20) admits in general four solutions $\pm k_1$, $\pm k_2$. The dispersion curves are shown in Fig. 1, the ratio of the ellipse's axes in Fig. 2, where the sign of the axes ratio defines the handedness of the elliptic polarization. To this purpose, we notice that the eigenmodes T_1^+ and T_2^+ have everywhere opposite signs, whereas similar plots in Ref. [7] show an interval where they have the same sign. This apparent discrepancy is simply due to a different labeling of the eigenmodes. Our labels + and − define the sign of the group velocity $d\omega/dk$ (that gives the direction of the energy flux), whereas in Ref. [7] the modes are labeled according to the sign of k. The apparent discrepancy occurs in the interval of the dispersion curves where k and $d\omega/dk$ have opposite signs.

Here and in Fig. 3 we assume elastic constants corresponding to the tetragonal crystal tellurium dioxide (class 422) where $C_{12}:C_{13}:C_{11}:C_{33}:C_{55}:C_{66}=5.12:2.18:5.5:10.587:2.65:6.59$ [16]. All the curves have the same shape as the curves obtained for the electromagnetic waves. In particular, the curves T_1^+ and T_1^- clearly show the well-known frequency gap, where *k is purely imaginary and the periodic structure gives a Bragg diffraction band*. The presence of a forbidden band has already been evidenced in Refs. [3] and [7]. Real and purely imaginary k values correspond to propagating waves (stable solutions) and to standing evanescent waves (*unstable solutions*), respectively. For what concerns the polarization of the eigenmodes, the most important property has already been evi-

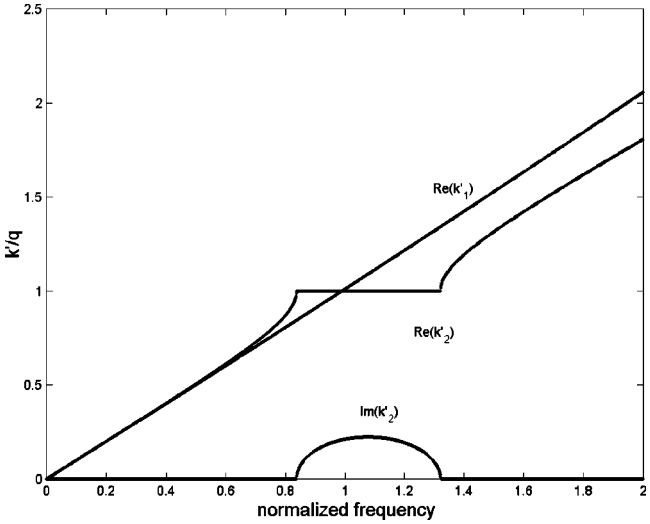

FIG. 3. Dispersion curves in the laboratory frame. The curves give the wave vectors of the dominant Fourier component of the Bloch waves T_1^+ and T_2^+. The material parameters are the same as in Fig. 1.

denced in Ref. [3] and can be stated as follows. The eigenmodes are in general elliptically polarized; in the rotating frame, the shape of the ellipse is independent of x_3; in the laboratory frame it rotates along x_3, rigidly following the rotation of the structure. A plot versus x_3 of the field components u_i' or σ_{ij}' in the laboratory frame, at a fixed instant t, gives beatinglike curves. This fact is obviously related to the presence of the two characteristic periods: the wavelength $\lambda = 2\pi/k$ and the period $p = \pi/q$ of the structure. Such properties are also displayed by the optical waves in cholesterics, but the acoustical waves give rise to a more rich variety of behaviors. In particular, a beating structure appears even in the L-modes if we consider the components σ_{11}', σ_{22}', and σ_{12}' of the stress tensor [3].

We add here the following interesting properties, valid for real values of the constants C_{55} and C_{66} (the case of complex elastic constant is discussed in Sec. III C).

(i) At the boundaries of the Bragg band, the eigenvalue k of the mode T_1^+ is equal to zero, and Eq. (19) gives

$$\frac{\omega_1^2}{\omega_2^2} = \frac{C_{66}}{C_{55}}. \tag{23}$$

The band width only depends on the anisotropy ratio C_{66}/C_{55} and could be very large.

(ii) If the solution is stable, one of the two ellipse's axes is everywhere along the symmetry axis of the structure. If it is unstable, the ellipse collapses into a straight line. The polarization is linear, with the vector $\vec{u}$ everywhere parallel to $x_1 \equiv z$ at one of the two boundaries of the forbidden band, obliquely oriented with respect to x_1 within the band, and parallel to x_2 at the other boundary: it therefore rotates of 90° for ω going from ω_1 to ω_2.

Such properties are immediately found by considering Eq. (21). The ratio u_2/u_1 is purely imaginary (a fact that obviously means elliptic polarization, with the ellipse's axes along x_1 and x_2) if k is real; it is real (and the polarization is linear) if k is purely imaginary; it is equal to zero or to infinite if $k = 0$.

For complex values of the constants C_{55} and C_{66}, the wave vector k is in general complex: the simplicity of the properties discussed here is therefore lost.

A. Acoustical rotation

The most important optical and acoustical properties of N^*-like systems for axial propagation are related to their rotatory power and to the presence of a single and very large forbidden band. In this section we consider the acoustical rotation. Since it has already been considered in Ref. [3], we only discuss its dependence on the ratio $k/q = p/\lambda$, where p is the pitch of the helical structure and λ the average wavelength of the eigenmodes T_1, T_2. This dependence appears in fact as quite complicated and very unusual, if compared with the one displayed by the homogeneous chiral crystals. We recall the following.

(i) Homogeneous crystals rotate the polarization plane of linearly polarized waves propagating along their acoustic axes, because in these directions the eigenmodes are circularly polarized in opposite senses and have different wave vectors k_1, k_2.

(ii) The rotatory power, i.e., the rotation ψ/d per unit length, is equal to $(k_2 - k_1)/2$ and scales as a/λ^2, where a is an average length of the lattice cell. Significant deviations from the λ^{-2} law are only found for λ of the order of a [17], i.e., in a frequency range where the medium is strongly dispersive.

To discuss the rotatory power of N*-like systems, we must find out k_i' $(i = 1,2)$ and the corresponding wave vectors $\vec{u}_i' = \underline{R}\vec{u}_i$ *in the laboratory frame* for the modes T_1^+, T_2^+. To this purpose, it is convenient to consider any eigenwave as a superposition of circularly polarized waves, because the transformation R leaves unchanged the polarization state of these waves and simply shifts their wave vectors from k to $k' = k \pm q$, where the sign depends on the handedness of the circular polarization. Any polarization state can be written as a superposition of left and right circularly polarized states by means of the Jones formalism:

$$\begin{pmatrix} a_1 \\ i a_2 \end{pmatrix} = \frac{a_1 + a_2}{2}\begin{pmatrix} 1 \\ i \end{pmatrix} + \frac{a_1 - a_2}{2}\begin{pmatrix} 1 \\ -i \end{pmatrix} = a_l\begin{pmatrix} 1 \\ i \end{pmatrix} + a_r\begin{pmatrix} 1 \\ -i \end{pmatrix}, \tag{24}$$

where a_l and a_r are, respectively, the amplitude of the left and of the right circular components. The difficulty to study the acoustical activity in N^*-like systems is related to the fact that in the laboratory frame the eigenmodes T_1^+ and T_2^+ are no more plane waves, but Bloch waves with two plane wave components having wave vectors $k_i' = k_i \pm q$, $i = 1,2$. Strictly speaking, such modes cannot give acoustical activity. However, a large p/λ range exists, where one of the two circular components is very small with respect to the other one and, as a first approximation, it can be neglected: the ellipse described by the vector $\vec{u}(t)$ at any given point is very close to a circle. This actually occurs in the low frequency range, and more precisely for p/λ' going from zero up to ~ 0.5, where λ' is the wavelength in the laboratory frame. In this range, the medium behaves in fact as homogeneous, at least for its acoustical and optical properties [18–20], since the period of the structure is small with respect to the wavelength. However, even in this range a great difference exists between chiral crystals and the N^*-like structure considered here, where the rotatory power ψ/d is given by

$$\frac{\psi}{d} = \frac{k_{\mathrm{int}}^4 \delta^2}{8q(k_{\mathrm{int}}^2 - q^2)} + O(\delta^4). \tag{25}$$

This equation is the acoustical equivalent of the de Vries equation [21]; it is easily derived from Eq. (20) by considering the dominant circular component of the eigenmodes T_1^+, T_2^+. For $p \ll \lambda'$, Eq. (25) gives a scaling low of the type k_{int}^4/q^3. The rotatory power scales as λ^{-4}, not as λ^{-2}. In fact k_{int}^4 is proportional to ω^4 [see Eq. (22)], to k'^4 (see Fig. 3), and therefore to λ'^{-4}.

At higher frequencies, the smaller components of the Bloch waves gradually increase, and give new and undesired effects, at least for the acoustical rotation: we have a *pseudo* rotatory power, where the rotation is no more uniform and a linearly polarized wave becomes slightly elliptical, with an oscillatory behavior of the smaller ellipse's axis. The average rotatory power is still given by $(k_2'-k_1')/2$, where k_1' and k_2' refer to the dominant Fourier components of the Bloch waves. As shown in Fig. 3, this quantity has maxima at the edges of the forbidden band, where the approximated formula (25) fails. Interestingly, the medium can give optical rotation even in the forbidden band, as explained in the next section. At a given value $\lambda'_{\mathrm{inv}} \approx p$ of λ' within this band, the rotatory power changes its sign. For $\lambda' > \lambda'_{\mathrm{inv}}$, the polarization plane rotates in the same sense as the symmetry axis of the helical structure, for $\lambda' < \lambda'_{\mathrm{inv}}$ it rotates in the opposite sense.

The undesired effects increase by increasing p, and for $p > \lambda'/\delta$ we are outside the pseudo rotatory power regime: for each one of the eigenmodes, the ellipse described by the vector $\vec{u}$ is strongly elongated, and a superposition of the two eigenmodes gives rise to a complicated space dependence of the vector $\vec{u}$. At higher p values, i.e., for $p \gg \lambda'/\delta$, the ellipse practically collapses into a straight line: the polarization of the T eigenmodes is nearly linear, with $\vec{u}$ parallel or orthogonal to the symmetry axis of the structure. The eigenmodes are guided by the structure, in the sense that their polarization plane simply rotates, adiabatically following the rotation of the elastic tensor (*adiabatic limit or waveguide regime* [22]). This rotation must not be confused with the rotatory power, because it only occurs for two well defined and mutually orthogonal input polarizations: all the other linearly polarized waves excite both eigenmodes, which travel at different phase velocities $(C_{66}/\rho)^{1/2}$ and $(C_{55}/\rho)^{1/2}$, giving in general elliptic output polarization.

B. Unstable solutions

The presence of a frequency band where the k value for a T-mode becomes purely positive imaginary, giving selective attenuation, has already been evidenced in Ref. [7]. We discuss here the possibility to obtain pseudo rotatory power even within the forbidden band, despite the fact that here the mode T_1 is linearly polarized. To this purpose, let us first describe the mechanism that gives rise to an unstable solution. Consider a lossless helical medium and an ideal setup made of a source sheet at the plane $x_3=0$, and of a perfect termination sheet at $z=d$, where the wave is totally absorbed. If the polarization state of the wave generated by the source is orthogonal to the polarization state of the mode T_2^+ (and therefore nearly circular) only the mode T_1^+ is excited. In the limit $d \to \infty$, the wave does not reach the termination sheet, because it is attenuated: this means that it is *gradually* but totally reflected by the successive layers of the medium. The linear polarization of the eigenmode T_1^+ comes from the superposition of the forwardly and backwardly propagating plane waves, that at any point are circularly polarized with the same amplitude and opposite senses of rotation, and give therefore rise to a linearly polarized standing wave. For small enough d values, the amplitude of the reflected wave is very small, and the wave generated by the source reaches the termination sheet practically unchanged, i.e., circularly polarized. In this condition, the wave generated by the source is no more a standing wave but a circularly polarized propagating wave, that can be considered as a superposition of the eigenmode T_1^+ and T_1^- (the presence of this last eigenmode is required by the boundary conditions at the termination sheet). It is now easily understood that within the forbidden band the sample gives selective attenuation or pseudo rotatory power, depending on its thickness.

The optical equivalent of the acoustical rotation within the forbidden band is well known: measurements of the optical rotatory power of cholesteric liquid crystal samples [23] and of chiral sculptured thin films [24] in the forbidden band have been done. We presume that the effect discussed here could also be of interest for acoustical applications, since in a limited frequency range the rotatory power goes continuously from positive to negative values, and can give an acoustical rotation of 90° along a path of few pitches.

Obviously the interest of the unstable solutions is not restricted to the acoustical rotation. A further reason of interest is evidenced in the next section. We conclude this section by considering the reflection properties of the helical structure for waves that only excite the eigenmode T_1^+. The polarization state of the external plane wave must be suitably selected; it is nearly circular if the impedance mismatch of the two media is very small. For such wave, a thick sample behaves as a perfect mirror, because it gives total reflection. However, the mirror and the helical medium give reflected waves with opposite handedness. This unusual reflection property of helical media is a consequence of the very particular reflection mechanism described above. In the mirror reflection the incident and the reflected waves have the same angular momentum. In the helical medium the angular momenta are opposite: if the first medium is a viscous anisotropic liquid (that supports viscous shear waves), a circularly polarized wave can rotate the reflecting helical structure.

C. Lossy media

The very simple polarization properties of the eigenmodes in lossless media have been derived by considering that all the quantities appearing in Eq. (21) are purely real or purely imaginary. In lossy media the elastic constants C_{55} and C_{66} become complex and the simplicity of the solutions is lost. All the eigenmodes show dissipative attenuation, that in the forbidden band adds to the reactive attenuation already discussed for lossless media. For perfect crystals the dissipative attenuation is very small, but in artificial structures a second and more efficient source of attenuation could be present, due to the defects that act as diffusing centers.

The attenuation due to absorption or diffusion (*extinction*) is generally considered as a parasitic effect, to be avoided at least for what concerns the working of instruments. However, it could give rise to a conceptually interesting new

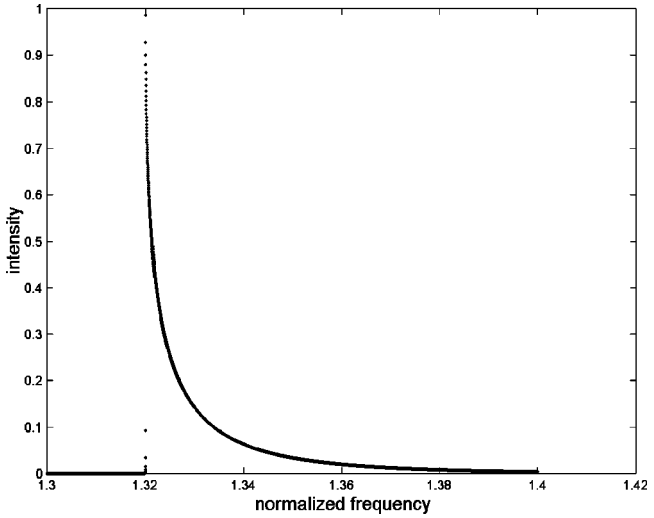

FIG. 4. Attenuation of the eigenmode T_1^+ over a distance $d=10^3\lambda_{\rm int}$, for a hypothetical medium with parameters values $C_{55}=2.65\times10^{10}$ and $C_{66}=(6.59+0.1\ i\omega)10^{10}$ in SI units. The wave is strongly attenuated except in a very thin interval ($\Delta\omega/\omega\sim0.01$), close to one of the boundaries of the forbidden band, that is at the left-hand side of the transmittance peak. The curve evidences an unusual and interesting property of the eigenwaves in proximity of the forbidden band.

effect, consisting in an anomalous transmission peak at one of the boundaries of the forbidden band (Borrmann effect). This fact is a consequence of the extinction anisotropy, and of the fact that at the two boundaries the polarization is nearly linear, with the polarization plane parallel or orthogonal to the symmetry axis of the structure, where the extinction is minimum or maximum. Obviously, the transmission peak corresponds to the case of minimum extinction. It could be very enhanced for strongly anisotropic attenuation, as shown by Fig. 4, where the ideal case of exactly zero attenuation for $\vec{u}$ parallel to the symmetry axis is considered. The Borrmann effect has been first found for x rays in 1941 [25], observed in cholesteric liquid crystals samples for light waves [26] and discussed in thin films helicoidal bianisotropic media for electromagnetic waves [27].

We finally observe that something similar to the reactive attenuation and to the Bragg reflection could also be present in the liquid phase of cholesterics, where the elastic stress tensor $\underline{\sigma'}$ is zero but the medium can support strongly attenuated shear waves, owing to the presence of a viscous stress tensor. A description of the viscous shear waves in anisotropic liquids is given in Ref. [22].

IV. AXIAL PROPAGATION IN SMECTICLIKE STRUCTURES

We consider here the helical structures where the transversal and longitudinal components of the acoustic wave are coupled. By suitably choosing the direction of the axes x_1, x_2, the submatrix $\underline{B}_{u\sigma}$ of the propagation matrix B can be written as

$$\underline{B}_{u\sigma}=-i\,\underline{\eta}=-i\begin{pmatrix}\eta_1 & 0 & \eta'\\ 0 & \eta_2 & \eta''\\ \eta' & \eta'' & \eta_3\end{pmatrix}, \tag{26}$$

and for lossless media it is real. The off-diagonal matrix elements η' and η'' act as coupling terms between the longitudinal and transversal components of the vector $\vec{u}$. This gives new effects, without an optical equivalent: hence the great interest of this case. In general, all the eigenwaves are now elliptically polarized. The ellipse described by the vector $\vec{u}$ at any given point rotates solidary with the symmetry axis without changing its shape, but it is contained in a plane obliquely oriented with respect to x_3. One of the main axes of the ellipse is along x_1 if $\eta'=0$, along x_2 if $\eta''=0$. If both η' and η'' are different from zero, the ellipse's axes can in principle have any direction.

From Eqs. (4), (10), and (26), the following bicubic dispersion relation is easily found:

$$k^6-k^4a+k^2b+c=0, \tag{27}$$

where

$$\begin{aligned}a&=(\eta_1+\eta_2+\eta_3)\rho\omega^2+2q^2,\\ b&=(\eta_1\eta_2+\eta_1\eta_3+\eta_2\eta_3-\eta'^2-\eta''^2)\rho^2\omega^4\\ &\quad+(2\eta_3-\eta_1-\eta_2)q^2\rho\omega^2+q^4,\\ c&=(-\eta_1\eta_2\eta_3+\eta_2\eta'^2+\eta_1\eta''^2)\rho^3\omega^6\\ &\quad+(\eta_1\eta_3+\eta_2\eta_3-\eta'^2-\eta''^2)\rho^2\omega^4q^2-\eta_3\rho\omega^2q^4.\end{aligned} \tag{28}$$

New forbidden bands, where k has an imaginary part, are expected. Since the roots $\pm k_1,\pm k_2,\pm k_3$ of Eq. (27) satisfy the relation

$$k_1^2+k_2^2+k_3^2=a>0, \tag{29}$$

the following cases can in principle appear, for real elastic constants:

(1) the three k_i^2 are real, and at least one is positive;

(2) only one of the k_i^2 values is real, the other two are complex conjugated.

As evident, real positive k_i^2 values correspond to stable solutions, real negative k_i^2 values correspond to unstable solutions with purely imaginary wave vectors. The possible couple of complex conjugated k_i^2 values gives four strictly related eigenmodes, with wave vectors $\pm k'\pm ik''$. Many different types of dispersion curves can appear, depending on the actual values of the elastic constants and of the helix pitch: the universal and simple behavior of the dispersion curves of N^*-like structures is lost. It is however to be observed that for small values of the coupling parameters η' and η'' the properties of the eigenmodes are in general not very far from the ones discussed in Sec. III. In this case, it is convenient to first find out the properties of the unperturbed eigenmodes, obtained by setting $\eta'=\eta''=0$. Only around the degeneration points the properties of the perturbed and

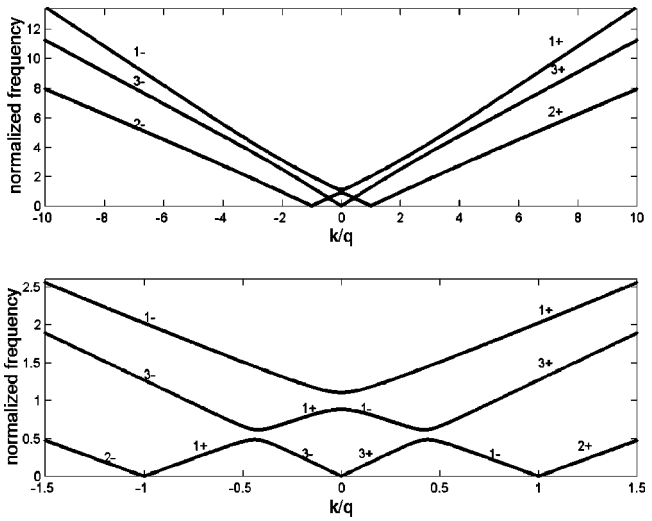

FIG. 5. Dispersion curves in the rotating frame for a smecticlike structure, made of tellurium dioxide, with $\theta=45°$.

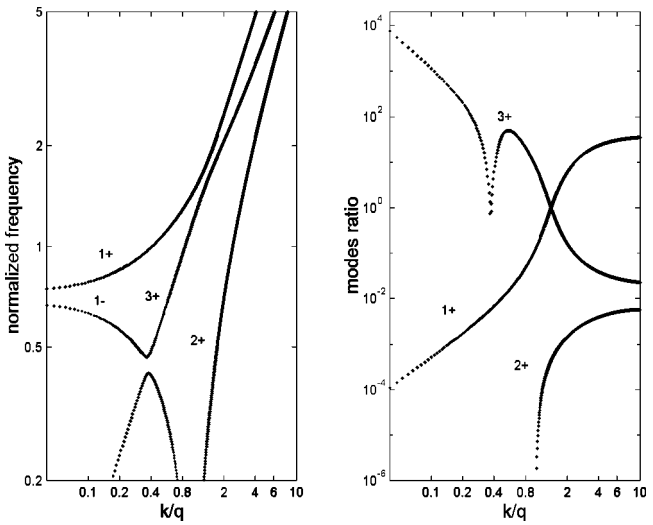

FIG. 6. Dispersion curves and modes ratio in the rotating frame for a smecticlike structure with $C_{11}:C_{33}:C_{13}:C_{44}:C_{55}:C_{66}=6:10:1:4:5:2$ and $\theta=45°$; the modes ratio is defined as $u_3^2/[u_1^2+u_2^2]$. It is equal to 0 and to ∞ for purely transversal and purely longitudinal modes, respectively.

unperturbed eigenmodes are very different. The typical behavior of the perturbed dispersion curves is plotted in Fig. 5. Such behavior, and the properties of the corresponding eigenmodes, can be understood on the basis of the following arguments. The unperturbed dispersion curves for the transversal modes are similar to the ones discussed in Sec. III and plotted in Fig. 1. In general, these curves are intersected by the dispersion curve of the longitudinal mode in two different points $k=k_1<q$ and $k=k_2>k_1$. At these points the unperturbed solutions are degenerated, but in the presence of the coupling terms the degeneration disappears and a *mode mixing* occurs. It is now easily understood, on the basis of simple topological and physical arguments, that the mode mixing gives a *new forbidden band* at the first one of the two intersection points, and a longitudinal to transversal mode exchange at the other one, without a further forbidden band. In fact:

(i) the unperturbed L^+-curve crosses the horizontal axis of Fig. 1 at $k/q=0$: it therefore first intersects the mode T_1^-. A mode mixing between two waves traveling in opposite direction gives rise to standing waves, and the degeneration point can be avoided only if a new forbidden band appears, for topological reasons;

(ii) the same L^+-curve can intersect again the curve T_1^+ or the curve T_2^+, depending on the parameter values. In any case, the two intersecting curves correspond to waves propagating in the same direction. Their mixing gives rise to new progressive waves, as evident, with a longitudinal to transversal mode exchange, and vice versa. The two positive unperturbed k_i^2 values are only slightly changed by the perturbation, and are still positive.

The perturbed dispersion curves corresponding to the case of unperturbed curves with degeneration points at $k_1\approx 0.4q$ and $k_2\approx 1.5q$ are plotted in Fig. 6, together with a quantity related to the ratio between the longitudinal and transversal components of the displacement vector $\vec{u}$. The perturbed dispersion curves never give a degeneration point because they never intersect. They clearly show the new *forbidden band*, corresponding to the first intersection point at $k=k_1$, and the longitudinal to transversal *mode exchange* at $k=k_2$, where the L and T components are nearly equal for each one of the eigenmodes T_1^+ and T_3^+. The parameter values are such that the unperturbed L-curve intersects the unperturbed T_1^+ and T_1^-, but not the curve T_2. This last transversal eigenmode remains therefore everywhere essentially transversal.

For C_{11} intermediate between C_{44} and C_{55} the second intersection point can be absent. In this case, the longitudinal to transversal mode exchange never occurs, as shown in Fig. 7.

A suitable choice of the parameters allows to obtain a strong mixing between any couple of components of the vector $\vec{u}$, a fact that could be of interest for applications (longi-

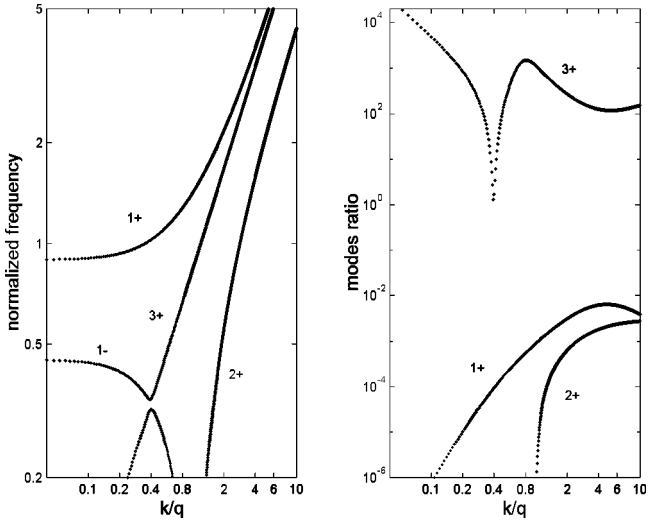

FIG. 7. The same as in Fig. 6 with $C_{11}:C_{33}:C_{13}:C_{44}:C_{55}:C_{66}=4.5:5.6:1:6:4:10$ and $\theta=45°$.

tudinal to transversal mode-exchange and acoustical rotation).

V. OBLIQUE PROPAGATION

If the wave vector of the incident wave is not parallel to the helix axis x_3, the propagation matrix $\underline{B}$ depends on x_3 even in the rotating frame, where the elastic constants are x_3 independent. The dependence on x_3 comes from the fact that in this frame the incident wave vector $\vec{k}'$ is seen to rotate. In both the laboratory and the rotating frames, the six eigenmodes are in general Bloch waves with an infinite number of Fourier components. Different formalisms have been developed for the study of the eigenmodes of the electromagnetic field in helical liquid crystals, based on recurrent relations [28] or on suitably truncated Fourier expansions [29,30].

More recently, a different formalism has been developed by Lakhtakia for the very general case of helical piezoelectric crystals, where 10 independent eigenmodes exist [5]. It is based on the expansion of the propagation matrix for the field components in a power series of x_3. The coefficients of the series, that are 10×10 matrices, are expressed as functions of the Fourier components of the kernel matrix appearing in the propagation equation. Since only five Fourier components are different from zero, their expressions are rather simple. In Ref. [6] the method has been extended to the case of media with sources. The method is particularly suitable for finite samples, because the series is very rapidly converging for small values of the ratio between the sample thickness and the helix pitch.

Since we are interested to the bulk properties of eigenmodes, most of the already developed methods are of little usefulness. Therefore, we only consider the case of quasiaxial propagation, where k_1' is small and the term depending on x_3 can be treated perturbatively.

The propagation matrix $\underline{B}$ is written as $\underline{B}=\underline{B}^{(0)}+\underline{B}^{(1)}(x_3)$, and $\underline{B}^{(1)}(x_3)$ is considered as a perturbation. A very interesting approximation is already obtained by fully neglecting the matrix $\underline{B}^{(1)}(x_3)$. This approximation is well known in optics, where it is referred as *quasinormal approximation* [29]. The matrix $\underline{B}^{(0)}$ is immediately obtained from Eqs. (5) and (6) by setting $\cos^2\phi=(1+\cos 2\phi)/2$ and $\sin^2\phi=(1-\cos 2\phi)/2$. The submatrices $\underline{B}^{(0)}_{uu}$, $\underline{B}^{(0)}_{u\sigma}$, and $\underline{B}^{(0)}_{\sigma\sigma}$ are exactly the same as for axial propagation, whereas in the matrix $\underline{B}^{(0)}_{\sigma u}$ a new term depending on k'^2_1 appears. The solutions of the propagation equations are similar to the ones found in the preceding sections and valid for axial propagation. Since the new term depends quadratically on k_1', it gives negligibly small effects at quasiaxial propagation. This fact is of great interest from the point of view of experiments, since the acoustical field contains in any case waves whose wave vector is not exactly parallel to the helix axis, owing to diffraction. Our analysis shows that a small transversal component of the wave vector gives in general very small effects.

Outside the limits of validity of the *quasinormal approximation*, the use of the rotating frame is in general no more convenient. We only observe that at oblique propagation the six independent solutions of the propagation equation are Bloch waves with an infinite number of Fourier components, and a numerical analysis is in general required.

VI. CONCLUSIONS

The optical properties of helical-shaped periodic media are well known and described in any textbook on liquid crystals. It seems therefore convenient to summarize and discuss the analogies and differences between optical and acoustical properties. As a first and very important point, we observe that the most interesting analogies are found by comparing the electromagnetic wave with the transversal components of the acoustic waves, related to shear deformations. This means that we must consider artificial helical media made of solid crystals, since liquid crystals do not support elastic shear waves. Artificial helical structures are easy to be prepared. The first one, made of thin mica sheets, has been prepared and studied before the discovery of liquid crystals. Now many other techniques are available [12,11]. Another possibility is to obtain the helical medium by simply freezing a liquid crystal sample. For the electromagnetic waves, the difference between liquid and solid structures is not very important, at least in the framework of linear optics, whereas it becomes essential for the acoustic waves.

The most important difference between optical and acoustical waves is due to the fact that in optics the possible longitudinal mode is generally of little practical interest: it becomes important only under very particular conditions (as for instance near dipolar or quadrupolar adsorption lines [31]). Obviously, the longitudinal component of the acoustic waves is never negligible, and it is generally coupled to the transversal ones. In helical media, the coupling terms go to zero only if the two following conditions are met: the helical structure is made of crystals having a symmetry axis orthogonal to the helix axis (cholestericlike structures), and the wave vector $\vec{k}$ is parallel to the helix axis (axial propagation). In this case, a very close analogy exists between the shear acoustic waves and the electromagnetic waves. It has been evidenced in Sec. III.

In Sec. IV, the case of axial propagation in smecticlike structures is considered, where the transverse and the longitudinal components of $\vec{u}$ are coupled. This is perhaps the most interesting case, and represents the most important result of our research. In fact, fully analytic and very simple solutions are found, without any optical analogue. At oblique propagation a numerical analysis or approximate methods are required for both optical and acoustical waves.

The research given here only concerns the bulk properties of the helical structures, but it evidences very interesting effects which could stimulate new applications, in addition to those already considered in Refs. [7–10].

APPENDIX A

The propagation equations in the laboratory frame x_1', x_2', x_3' are

$$-\rho\omega^2 u_i' = \partial_i' \sigma_{ij}', \quad \sigma_{li}' = \lambda_{lijm}' \partial_j' u_m', \tag{A1}$$

where $\partial'_j = \partial/\partial x'_j$, and admit solution of the type

$$u'(\vec{x}') = u'_i(x'_3)\exp(ik'_1x'_1), \quad \sigma'_{ij}(\vec{x}') = \sigma'_{ij}(x'_3)\exp(ik'_1x'_1). \tag{A2}$$

The corresponding equations in the rotating frame are immediately found by setting

$$u'_{i'} = R_{i'i}u_i, \quad \sigma'_{i'j'} = R_{i'i}R_{j'j}\sigma_{ij},$$

$$\lambda_{i'j'l'm'} = R_{i'i}R_{j'j}R_{l'l}R_{m'm}\lambda_{ijlm}, \tag{A3}$$

where $\underline{R} = \exp(\underline{r}\phi)$, and taking into account the relations

$$\partial'_1 = ik'_1, \quad \partial'_2 = 0, \quad \partial'_3 = \partial_3, \tag{A4}$$

$$\partial_3 R_{ij} - R_{ij}\partial_3 = qr_{ik}R_{kj},$$

$$R_{ik}R_{jk} = R_{ki}R_{kj} = \delta_{ij},$$

$$R_{3l}r_{lm} = r_{3m}, \quad r_{3l} = 0.$$

With the symbols of Sec. II, the propagation equations can be written as

$$-\rho\omega^2 u_i = ik'_1(\sigma_{i1}\cos\phi - \sigma_{i2}\cos\phi) + qr_{ik}\sigma_{k3} + \partial_3\sigma_i, \tag{A5}$$

$$\sigma_{i3} = [ik'_1(\tilde{\lambda}^{31}_{im}\cos\phi - \tilde{\lambda}^{32}_{im}\sin\phi) + q\tilde{\lambda}^{33}_{ik}r_{km}]u_m,$$

$$\sigma_{ij} = [ik'_1(\tilde{\lambda}^{j1}_{im}\cos\phi - \tilde{\lambda}^{j2}_{im}\sin\phi) + q\tilde{\lambda}^{j3}_{ik}r_{km} + \tilde{\lambda}^{j3}_{im}\partial_3]u_m,$$

where the index j in the last equation only assume the values 1 and 2. Such equations are fully equivalent to Eqs. (4),(5), and (6) given in the text, that are simply written in a more compact form.

[1] A. Lakhtakia, J. Acoust. Soc. Am. **95**, 597 (1994); **95**, 3669(E) (1994).
[2] S. Ponti, K. Zvezdin, M. Scalerandi, V. Agostini, and C. Oldano, in *Review of Progress in Quantitative Nondestructive Evaluation*, edited by D.O. Thompson and D.E. Chimenti (American Institute of Physics, New York, 2000), p. 177.
[3] S.F. Nagle, A. Lakhtakia, and W.J. Thompson, J. Acoust. Soc. Am. **97**, 42 (1995).
[4] A. Lakhtakia, Appl. Acoust. **44**, 25 (1995); **44**, 385(E) (1995).
[5] A. Lakhtakia, Appl. Acoust. **49**, 225 (1996).
[6] A. Lakhtakia, K. Robbie, and M.J. Brett, J. Acoust. Soc. Am. **101**, 2052 (1997).
[7] S.F. Nagle and A. Lakhtakia, Sens. Actuators A **49**, 195 (1995), **55**, 229(E) (1996).
[8] S.F. Nagle and A. Lakhtakia, Sens. Actuators A **55**, 139 (1996).
[9] A. Lakhtakia and W. Thompson, Jr., Sens. Actuators A **58**, 67 (1997).
[10] A. Lakhtakia and M. W. Meredith, Sens. Actuators **73**, 195 (1999).
[11] A. Lakhtakia and R. Messier, Mater. Res. Innovations **1**, 145 (1997).
[12] R. Messier and A. Lakhtakia, Mater. Res. Innovations **2**, 217 (1999).
[13] T. Motohiro and Y. Taga, Appl. Opt. **28**, 2466 (1989).
[14] N. Cherradi, A. Kawasaki, and M. Gasik, Composites Eng. **4**, 883 (1994).
[15] E. Reusch, Ann. Chim. Phys. **18**, 628 (1869).
[16] B.A. Auld, *Acoustic Fields and Waves in Solids* (Wiley Interscience, New York, 1984).
[17] Y.-J. Li and L. Chen, Phys. Rev. B **36**, 9507 (1987).
[18] C. Oldano and M. Rajteri, Phys. Rev. B **54**, 10 273 (1996).
[19] M. Becchi, C. Oldano, and S. Ponti, J. Opt. A: Pure Appl. Opt. **1**, 713 (1999).
[20] S. Ponti, C. Oldano, and M. Becchi (unpublished).
[21] H. de Vries, Acta Crystallogr. **4**, 219 (1951).
[22] P.G. de Gennes and J. Prost, *The Physics of Liquid Crystals*, 2nd ed. (Oxford Science, Clarendon, Oxford, 1993).
[23] S. Chandrasekhar, G.S. Ranganath, and K.A. Suresh, Proceedings of the ILCC, Bangalore, 1973; Pramana Suppl. **1**, 341 (1975); K.A. Suresh, Mol. Cryst. Liq. Cryst. **35**, 267 (1976).
[24] I. Hodgkinson, Q.H. Wu, B. Knight, A. Lakhtakia, and K. Robbie, Appl. Opt. **39**, 642 (2000).
[25] G. Borrmann, Z. Phys. **42**, 157 (1941); P.P. Ewald, Rev. Mod. Phys. **37**, 46 (1965).
[26] R. Nityananda, U.D. Kini, S. Chandrasekhar, and K.A. Suresh, Proceedings of the ILCC, Bangalore, 1973; Pramana Suppl. **1**, 325 (1975).
[27] V.C. Venugopal and A. Lakhtakia, Opt. Commun. **145**, 171 (1998); **161**, 370(E) (1999).
[28] M.A. Peterson, Phys. Rev. A **27**, 520 (1983).
[29] C. Oldano, Phys. Rev. A **31**, 1014 (1985).
[30] C. Oldano, E. Miraldi, and P. Taverna Valabrega, Phys. Rev. A **27**, 3291 (1983).
[31] V.M. Agranovich and V.L. Ginsburg, *Crystal Optics with Spatial Dispersion and Excitons* (Springer-Verlag, Berlin, 1984).